Nanoscale

COMMUNICATION

View Article Online
View Journal | View Issue

Facile graphene transfer directly to target substrates with a reusable metal catalyst†

D. L. Mafra, T. Ming and J. Kong*

Cite this: *Nanoscale*, 2015, **7**, 14807

Received 12th June 2015,
Accepted 1st August 2015

DOI: 10.1039/c5nr03892h

www.rsc.org/nanoscale

High-throughput, roll-to-roll growth and transferring of high-quality, large-area chemical vapor deposited (CVD) graphene directly onto a target substrate with a reusable metal catalyst is an enabling technology for flexible optoelectronics. We explore the direct transfer *via* hot lamination of CVD graphene onto a flexible substrate, followed by electrochemical delamination (bubble transfer) of the graphene. The transfer method investigated here does not require any intermediate transfer layer and allows the copper to be reused, which will reduce the production cost and avoid the generation of chemical waste. Such integration is one necessary step forward toward the economical and industrial scale production of graphene. Our method bares promise in various applications. As an example, we fabricated flexible solution-gated graphene field-effect-transistors, which exhibited transconductance as high as 200 μS.

Graphene, due to its unique electrical, mechanical, optical and thermal properties[1], shows promise in various applications, including photonics, optoelectronics, and organic electronics such as solar cells, light-emitting diodes, touch screen technologies, photodetector devices, and membranes for molecular separations in gases or liquids.[2–4] To be able to utilize raw materials for those applications, continuous production of graphene at high quality and low cost on arbitrary surfaces is desired, but yet to be achieved. The most common way is to grow chemical vapour deposited (CVD) graphene on top of a metal catalyst surface followed by transferring the graphene onto the target substrate.[5,6] During the transfer, an intermediate membrane, such as polymethylmethacrylate (PMMA), is spin-coated onto the graphene/metal surface. Afterwards, the metal is chemically etched away and the PMMA/graphene membrane is placed onto the target substrate. Finally, the PMMA is either removed *via* high-temperature annealing (~350–500 °C) or dissolved in acetone (or acetone vapour).[5,6] It has been commonly found that there are always PMMA residues on the graphene, which are hard to completely remove.[7–9] Furthermore, etching away the metal catalyst dramatically increases the graphene production cost and generates chemical waste. Other graphene transfer techniques have been investigated, including using thermal release tape as the transfer membrane;[4] directly transferring onto poly-dimethylsiloxane (PDMS);[10] using electrolysis to detach the graphene from the metal catalyst surface,[11–13] *etc*. Nevertheless, these techniques either use an intermediate membrane or need to chemically etch the metal catalyst.

In this work, we explored a transfer technique that abandons both an intermediate membrane and chemical etching of the metal catalyst. Our method combines the hot lamination of the target substrate onto the graphene/metal surface, as proposed by Martins *et al.*,[14] followed by the electrolytic delamination of graphene from the metal catalyst surface, as proposed by Wang *et al.*[11] and Gao *et al.*[12] The graphene is directly transferred onto the target surface and the metal catalyst can be used again for graphene growth. More importantly, we envision that combining the two methods is a necessary route towards the roll-to-roll production of large-area CVD graphene sheets at high quality and low cost. Fig. 1a illustrates our design in a roll-to-roll manner, where the flexible polymer film serves as the target substrate. The laminator temperature is set higher than the glass transition temperature of the polymer film, so that the surface of the polymer can deform and adhere closely to the graphene under lamination.[14] The metal/graphene/polymer sandwich structure was then immersed in an alkaline aqueous electrolyte, where the metal serves as the cathode for water electrolysis and for the hydrogen evolution reaction (HER). The electrode reaction is expressed as $2H_2O(l) + 2e^- \rightarrow H_2(g) + 2OH^-(aq)$. H_2 bubble generation at the copper surface gradually detaches the graphene from the copper but barely affects the graphene/polymer adhesion, therefore achieving the transfer of graphene to the flexible polymer substrate. The metal catalyst foil can be recycled in its original form and shape and it can be used for the next cycle of CVD graphene growth.

Department of Electrical Engineering and Computer Sciences, Massachusetts Institute of Technology, Cambridge, MA 02139-4307, USA. E-mail: jingkong@mit.edu

†Electronic supplementary information (ESI) available. See DOI: 10.1039/c5nr03892h

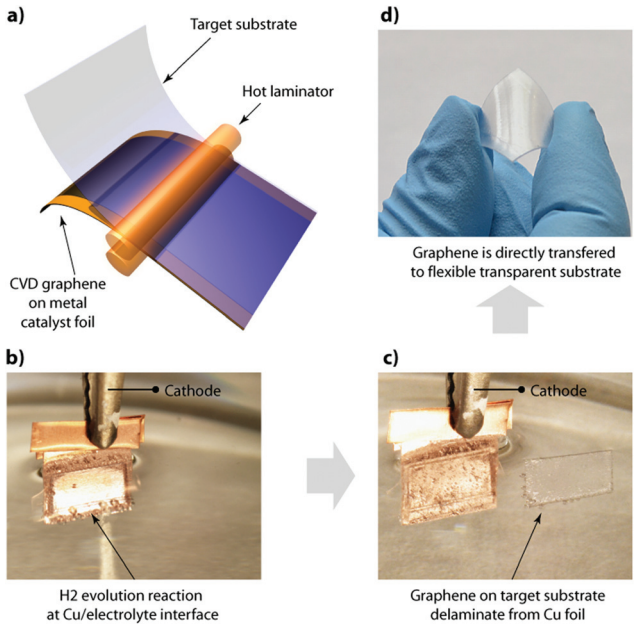

Fig. 1 (a) Schematic diagram of the transfer process. Graphene grows on both sides of the copper substrate and the graphene/copper/graphene (G/Cu/G) is placed on the target substrate (PVC). The substrate is inserted into the hot lamination machine for the adhesion of graphene on PVC. (b) After lamination, the PVC/G/Cu is connected as a cathode for electrochemical delamination. The substrate is completely immersed in the solution. (c) After the delamination is complete the PVC/graphene detaches from the Cu foil. At the end of the process we have the graphene layer on the PVC. The Cu foil can be recycled to grow graphene again. (d) The final sample of graphene on PVC.

We demonstrated our design experimentally using CVD graphene on Cu foil as the starting material (see ESI†). It is important to note that in principle all other metals demonstrated for graphene growth[5,15–19] can be used for the electrochemical exfoliation because this method relies on the electrolysis of H_2O to generate H_2. Here we use Cu foil since it is the most commonly used for graphene growth and it is also low cost. Briefly, the CVD graphene growth was carried out at 1000 °C for 30 minutes under H_2 = 70 sccm and CH_4 = 4 sccm flow. Polyvinyl chloride (PVC) film was chosen as the target substrate in this case for its high flexibility, good transparency and wide accessibility. Hot lamination was conducted at a roller temperature of 150 °C. For the electrolytic delamination of graphene, −5 V was applied to the Cu foil. Sodium hydroxide was used to make the aqueous electrolyte for its inertness towards electrolysis. The close contact between the PVC and the Cu/graphene prevents water from immediate penetration in between the layers. At the beginning of the delamination, bubbles form on the Cu at the edges of the PVC as shown in Fig. 1b. In a few minutes, bubbles start to form towards the center area in between the Cu and PVC stack. This suggests that water has penetrated from the edge towards the center. After the graphene/PVC sheet detaches from the Cu foil, it floats on the electrolyte surface and hydrogen bubbles evolve from the entire surface of the Cu foil (Fig. 1c). Graphene coated PVC obtained in this method is conductive, transparent and flexible (Fig. 1d). The hot lamination/electrolyte delamination method can also be extended to transfer graphene onto other polymer film substrates and the procedure is similar to that of PVC described above.

To study the quality of the graphene after electrolytic delamination, we first use PMMA film to transfer graphene onto a SiO_2/Si wafer with 300 nm thick SiO_2. Using a SiO_2/Si wafer allows the observation of the transferred graphene by optical microscopy and AFM (in contrast, monolayer graphene on PVC is difficult to observe under optical microscopy, Raman spectroscopy and AFM due to the low optical contrast, high interference Raman signal from PVC, and the rough polymer surface, respectively). The PMMA film is removed by thermal annealing at 500 °C under Ar = 400 sccm and H_2 = 700 sccm flow for 2 hours. The final monolayer graphene on SiO_2/Si is visible and uniform under the naked eye (Fig. 2a). The optical images (Fig. 2b and c) display a continuous graphene film and the AFM image reveals wrinkle features with an average unwrinkled domain size of 1 mm (Fig. 2d). The Raman spectrum exhibits a 2D/G peak ratio of 1.7, indicating monolayer graphene, and the low D band indicates low defect concentration (Fig. 2e).[20] The AFM and Raman characterizations were taken at different locations across the samples and similar results were observed. Those results indicate that despite the punchy lamination and vigorous bubbling, the continuity and integrity of the graphene sheet was preserved, which can be attributed to the close adhesion between the graphene and the PMMA film. A better graphene quality after the electrochemical transfer using polymer films with better adhesion with graphene is expected.

In previous electrochemical delamination studies in the literature,[11,12] either potassium sulfate (K_2SO_4) or sodium hydroxide (NaOH) aqueous solution was used as the aqueous electrolyte and very different concentrations were used (0.1 mM for ref. 11 *vs.* 1 M for ref. 12), but it is unclear which condition is better for the delamination. To optimize the electrolytic delamination and pursue better graphene quality after transfer, we studied the effect of different electrolyte solutions, electrolyte concentrations, and electrolytic potentials on the sheet resistance (R_{sq}) of the graphene. The results are summarized in Table 1. For this optimization, PMMA is used as a protective layer and the graphene was transferred to a SiO_2/Si substrate. Also, the graphene was grown on a pre-annealed Cu foil (details about the pre-annealing will be given later in the text). Both K_2SO_4 and NaOH solutions were investigated. Noticeably, the sheet resistance reveals the continuity and integrity of the graphene sheet after transfer. In general, 10 mM NaOH shows the best performance among all the experimental conditions, indicated by the low sheet resistance of $R_{sq} = 530 \pm 45\ \Omega\ \square^{-1}$.

Decreasing the NaOH concentration to 1 mM generates an incomplete graphene sheet (Fig. S1†) with a dramatically enlarged sheet resistance of 26 kΩ $\square^{-1}$. We believe that the breakdown of the graphene sheet during electrolysis for the low concentration solution is due to the slow and non-uniform

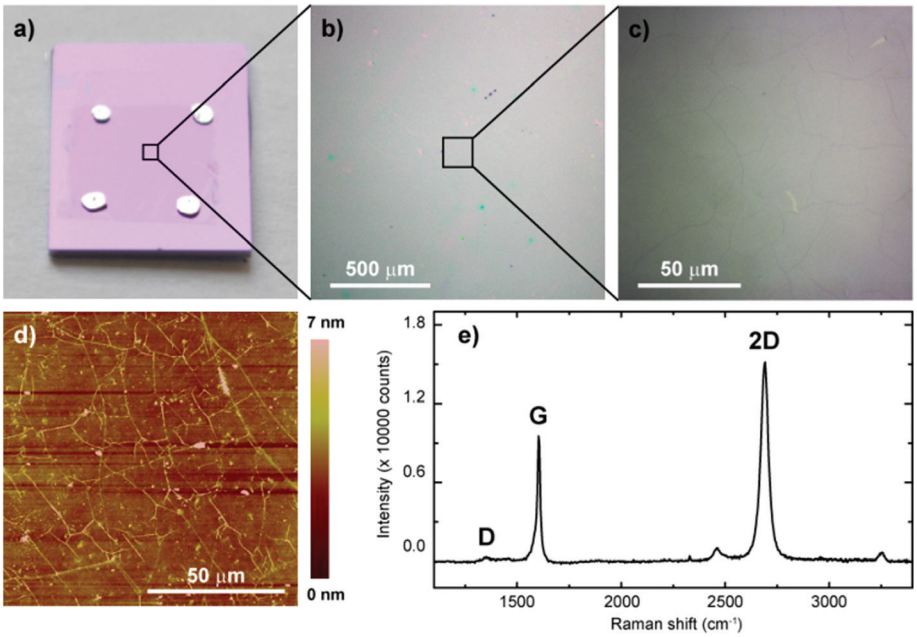

Fig. 2 (a) Picture of the graphene on the Si/SiO_2 substrate after the electrochemical delamination process using PMMA and 10 mM NaOH electrolyte with a 5 V power supply. (b, c) Optical images of the graphene on the Si/SiO_2 substrate showed in (a). (d) AFM image and (e) Raman spectrum taken with a 532 nm laser line of the graphene on Si/SiO_2 showed in (a).

Table 1 Sheet resistance (R_{sq}) of CVD graphene transferred by electrochemical delamination (bubble transfer) using different electrolytes, concentrations of solution and voltages

Electrolyte	Concentration [mM]	Voltage [V]	R_{sq} [$\Omega\ \square^{-1}$]	Time [~min]
K_2SO_4	0.1	5	—	90
		10	—	60
	1	5	—	30
		10	12 800–14 800	15
	10	5	700–960	5
		10	940–1110	2
	50	5	1300–3000	2
		10	1350–1420	2
NaOH	0.1	5	—	90
		10	—	60
	1	5	—	20
		10	25 547	10
	10	5	480–575	5
		10	449–627	3
	50	5	697–770	2
		10	824–1099	2

bubble generation at the Cu surface under low ionic conductivity.

Under strong electrolyte condition, the solute completely, or almost completely, ionizes or dissociates in a solution, which is the case of NaOH; 1 mM NaOH exhibits an ionic conductivity of 0.025 Sm. The low electrolyte conductivity leads to a low HER current and slow H_2 bubble generation, which results in individual, isolated bubbles on the Cu surface. More importantly, during the generation and expansion, each of the isolated H_2 bubbles introduces a non-uniform strain to the graphene sheet at the corresponding location. We assume that the non-uniform strain gives rise to tears and broken regions in the graphene. On the contrary, for higher NaOH concentration with higher ionic conductivity, the HER is faster and the isolated bubbles merge with each other to form a uniform gas layer. Increasing the NaOH concentration from 10 to 50 mM gives rise to vigorous bubbling and slightly increases the graphene sheet resistance from $530 \pm 45\ \Omega\ \square^{-1}$ to $730 \pm 40\ \Omega\ \square^{-1}$. It is worth noticing that increasing the electrolytic voltage from 5 V to 10 V speeds up the delamination process, which is due to faster hydrogen gas evolution. However the reproducibility of the result under 5 V appears to be better than that carried out under 10 V, as can be seen in the spread of the R_{sq} in Table 1.

The results for the K_2SO_4 electrolyte have a similar trend as those for NaOH, with slightly higher sheet resistances at corresponding conditions. As a reference, we did a traditional transfer of graphene using a PMMA and Cu etchant using the same graphene, and the sheet resistance in this case was R_{sq} = $545\ \Omega\ \square^{-1}$, which is very similar to the results obtained using electrochemical delamination with the optimized condition, showing the high quality of the electrolytic transfer. It is also worth mentioning that the sheet resistance value ($500\ \Omega\ \square^{-1}$) obtained for the optimized condition using the electrochemical delamination process is much lower than the value reported in the literature so far (~2 $k\Omega\ \square^{-1}$).[11] With the optimized conditions here, the delamination time is only 2–5 min, much faster than the Cu etching (20 min), which is very important for large scale production of graphene.

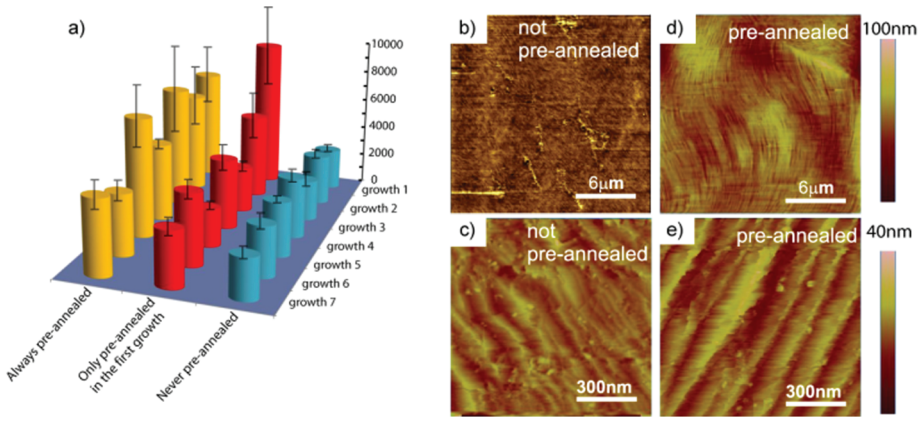

Fig. 3 (a) Dependence of the sheet resistance of the CVD graphene transferred to PVC on the number of regrowths using the same Cu foil pieces consecutively. The values are the average of the R_{sq} of five samples and the error bars are the standard deviation. Yellow cylinders show the dependence when the Cu foil pieces were pre-annealed before the growth and before each regrowth. Red cylinders show the results for the Cu foil pieces pre-annealed for only the first growth, and for consecutive regrowths no pre-annealing was carried out. Finally, for the blue cylinders, no pre-annealing was carried out in any step. (b, c) AFM images of the CVD graphene on the Cu foil. Cu/G surface for a not pre-annealed sample and (d, e) for a pre-annealed sample showing the formation of the Cu steps. The 100 nm height scale bar is for (b, d) and the 40 nm height scale bar is for (c, e).

The reuse of the metal catalyst is crucial in the large scale roll-to-roll production of CVD graphene since it can dramatically reduce the production cost and avoid generation of harmful chemical waste. In the pioneer work of Wang *et al.*[11] Cu was recycled three times and the graphene quality was maintained or even improved. Nevertheless, the graphene was transferred using PMMA onto SiO_2/Si substrates. Here we explored the recyclability of the Cu foil when transferred onto PVC directly. We cycle the growth/transfer procedure for five different samples and for seven times on the same piece of Cu foil and the R_{sq} of the obtained graphene on the PVC substrates was measured (Fig. 3a). The sheet resistance was kept constant at ~2.5 kΩ $\square^{-1}$ for each cycle (blue cylinders in Fig. 3a, where the values are the average of the R_{sq} of the five samples and the error bars are the standard deviation), which demonstrated the consistency of our method and the reusability of the metal catalyst in our case. The higher R_{sq} of the graphene transferred to the PVC substrate compared to those for the SiO_2/Si substrate can be attributed to several factors, such as the roughness of the PVC and the incomplete contact between the graphene/PVC interfaces. In the case of the PMMA transfer, PMMA solution is spin-coated onto graphene as a liquid, which ensures a complete close contact between the graphene and PMMA interface. During electrolytic delamination, the PVC cannot catch the graphene as tightly and uniformly as the PMMA, increasing the chance of tears in the graphene.

Previous studies have shown that the surface morphology of the metal catalyst affects the growth and transfer of the CVD graphene.[11] It was demonstrated that by pre-annealing the metal catalyst, its surface morphology can be modified and the quality of the graphene can be improved. These results were obtained using PMMA as the protective layer for bubble transfer. We have confirmed such results when carrying out the bubble-transfer of graphene using PMMA, but have found the opposite behavior when directly transferring the graphene to PVC substrates. In our method, for each new cycle of graphene growth/transfer, the Cu foil inevitably inherits the historical state after the previous cycle. It is important to track the surface morphology of the Cu foil after each cycle and to understand its impact on the next. Fig. 3b and c show the typical AFM image of the Cu foil after a growth/transfer cycle. It shows terraces with ~10 nm step heights between the crystal grains. By pre-annealing the Cu foil at 960 °C for 8 h under 50 sccm H_2 flow and cooling down to room temperature slowly at 30 °C h^{-1}, we are able to increase the Cu grain sizes and enlarge the step heights to ~30 nm (Fig. 3d and e). Pre-annealed Cu foil was used as the starting metal catalyst for the graphene growth/transfer. The process was also repeated for five samples and for seven cycles on each sample, and the sheet resistance of the obtained graphene on the PVC substrate for each cycle was measured (red cylinders in Fig. 3a). It is interesting that from the first cycle, the graphene sheet resistance is in the order of 10 kΩ $\square^{-1}$; while that from the second cycle shows a decreased sheet resistance of 4.5 kΩ $\square^{-1}$. Starting from the third cycle, the graphene sheet resistance was kept at ~2.6 kΩ $\square^{-1}$, which is similar to that without any pre-annealing in the Cu foil (blue cylinders in Fig. 3a). The CVD graphene growth and transfer processes reduce the surface roughness of the Cu surface.[11] The lower roughness facilitates the graphene adhesion to the PVC surface during hot lamination, therefore improving the quality of the graphene after its transfer. To further verify our hypothesis, we pre-annealed the Cu foil before every cycle. The average sheet resistance of the graphene for each cycle varies between 5 and 9 kΩ $\square^{-1}$ (yellow cylinders in Fig. 3a). In addition to this, we have also found that the samples with pre-annealing have much larger R_{sq} variation from sample to sample. Considering

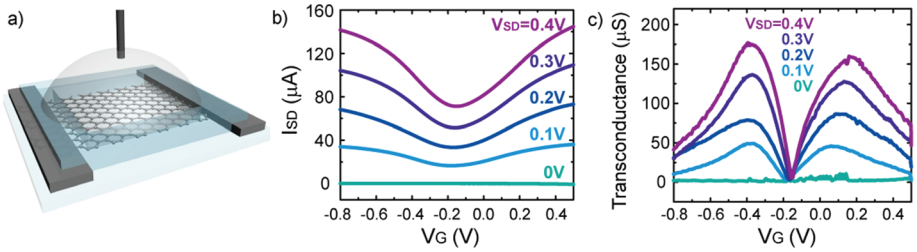

Fig. 4 (a) Schematics of the solution-gated graphene field-effect transistors (SGGFETs). (b) Source–drain current (ISD) as a function of the gate voltage VG of a top gated graphene device on PVC for different source–drain voltages (VSD). (c) Transconductance of the respective device as a function of the VG.

that the annealing brings up the Cu surface step height before each cycle, the correlation between the high surface roughness and high graphene sheet resistance confirms our hypothesis. The study here indicates that if a lamination process is used to directly transfer the graphene to a flexible substrate, pre-annealing should not be used to avoid roughening of the Cu surface. It was also found that the graphene growth and transfer cycle is self-adapting, *i.e.*, even if pre-annealing is carried out in the beginning (shown by the red cylinders in Fig. 3a) and poor graphene sheet resistance was obtained, improved graphene transfer was achieved after several cycles as the Cu roughness was reduced after each cycle.

The fact that the never pre-annealed samples have higher quality when compared to the pre-annealed ones is very interesting, since the opposite result is found when PMMA is used in the electrolytic delamination (the electrochemical delamination performed on a graphene sample grown on a not pre-annealed Cu foil gives a sheet resistance in the order of 5500 $\Omega\,\square^{-1}$). We believe that the high steps created by the pre-annealing treatment on the Cu foil create a guide for the bubbles to penetrate between the interface graphene/Cu foil, helping the delamination process. However when the graphene is hot laminated onto the PVC, this guide is not necessary since the Cu/graphene/PVC stack system is completely immersed in the electrolyte solution instead of being gradually immersed, as for using a PMMA film.

Our graphene transfer technique directly transfers CVD graphene to a flexible and transparent substrate, from which functional electronics can be built on. To further evaluate the electrical performance of those graphene sheets and their application potential, solution gated graphene field-effect transistors (SGGFETs) were fabricated as shown in Fig. 4a. Phosphate buffered saline (PBS) solution was used as the electrolyte for the top gate solution. This was used to mimic an environment in biomedical sensing and diagnosis. The transfer curves of a representative SGGFET device are presented in Fig. 4b. All transfer curves exhibit a minimum in the current at a gate voltage of $V_G = -0.17 \pm 0.01$ V, which corresponds to the Dirac point. Furthermore, Fig. 4b shows that the transistor current can be modulated by at least a factor of two. The source–drain current (I_{SD}) exhibits some degree of saturation for a $V_G = 0.4$ V away from the Dirac point, which is attributed to the contribution of the access resistance intrinsic to the device design. Fig. 4c depicts the transconductance of the device which is defined as the first order derivative of the I_{SD} with respect to the V_G. This parameter, which corresponds to the device sensitivity, is of special importance for sensor applications: it reflects the resulting change in the current for a small variation in V_G. Notably, the device possesses a maximum transconductance of 180μS, comparable to the state-of-the-art SGGFETs,[21,22] implying its high sensitivity when compared to the commonly used Si- or AlGaN-based devices.

Conclusions

In summary, we have demonstrated the direct transfer of CVD graphene from a metal catalyst to a target substrate using the combination of hot lamination and electrolytic delamination. Such a method neither uses an intermediate film that needs to be removed afterwards, nor etches the metal catalyst chemically. More importantly, it enables the recyclability of the metal catalyst for graphene production, therefore dramatically reducing the production cost and generation of chemical waste. We found an optimized condition of 10 mM NaOH electrolyte concentration for the delamination under an electrolytic voltage of 5 V and our optimized condition shows a better sheet resistance and a faster delamination, when compared to the results shown in the literature so far. It is revealed that for PVC as target substrate, the procedure is self-adapting for the Cu foil surface. No extra treatment to the Cu foil is needed after a cycle of CVD graphene growth and transfer, and the Cu is ready for the next cycle right away. Sensors and other electronic devices can be easily built based on the graphene transfer to flexible and transparent substrates using our method. We demonstrate a solution-gated graphene field-effect transistor that exhibits state-of-the-art performance.

Acknowledgements

The author D.L.M. thanks the financial support of the Brazilian agency CNPq for carrying out the graphene growth, electrochemical delamination and sheet resistance measurements. T.M. acknowledges support for graphene transistor fabrications, transconductance and mobility measurements as part of the Center

for Excitonics, an Energy Frontier Research Center funded by the U.S. Department of Energy, Office of Science, Basic Energy Sciences (BES) under award number: DESC0001088.

References

1 A. K. Geim and K. S. Novoselov, *Nat. Mater.*, 2007, **6**, 183.
2 F. Bonaccorso, Z. Sun, T. Hasan and A. C. Ferrari, *Nat. Photonics*, 2010, **4**, 611.
3 K. S. Kim, Y. Zhao, H. Jang, S. Y. Lee, J. M. Kim, J. H. Ahn, P. Kim, J. Y. Choi and B. H. Hong, *Nature*, 2009, **457**, 706.
4 S. Bae, H. Kim, Y. Lee, X. Xu, J. Park, Y. Zheng, J. Balakrishnan, T. Lei, H. R. Kim, Y. Song, Y. Kim, K. Kim, B. Ozyilmaz, J. Ahn, B. Hong and S. Iijima, *Nat. Nanotechnol.*, 2010, **5**, 574578.
5 A. Reina, X. Jia, J. Ho, D. Nezich, H. Son, V. Bulovic, M. S. Dresselhaus and J. Kong, *Nano Lett.*, 2009, **9**, 3035.
6 S. Bhaviripudi, X. Jia, M. S. Dresselhaus and J. Kong, *Nano Lett.*, 2010, **10**, 4128.
7 C. Gong, H. C. Floresca, D. Hinojos, S. McDonnell, X. Qin, Y. Hao, S. Jandhyala, G. Mordi, J. Kim, L. Colombo, R. S. Ruoff, M. J. Kim, K. Cho, R. M. Wallace and Y. J. Chabal, *J. Phys. Chem. C*, 2013, **117**, 23000.
8 A. Pirkle, J. Chan, A. Venugopal, D. Hinojos, C. W. Magnuson, S. McDonnell, L. Colombo, E. M. Vogel, R. S. Ruoff and R. M. Wallace, *Appl. Phys. Lett.*, 2011, **99**, 122108.
9 J. W. Suk, W. H. Lee, J. Lee, H. Chou, R. D. Piner, Y. Hao, D. Akinwande and R. S. Ruoff, *Nano Lett.*, 2013, **13**, 1462.
10 Y. Lee, S. Bae, H. Jang, S. Jang, S.-E. Zhu, S. H. Sim, Y. I. Song, B. H. Hong and J.-H. Ahn, *Nano Lett.*, 2010, **10**, 490.
11 Y. Wang, Y. Zheng, X. Xu, E. Dubuisson, Q. Bao, J. Lu and K. P. Loh, *ACS Nano*, 2011, **5**, 9927.
12 L. Gao, W. Ren, H. Xu, L. Jin, Z. Wang, T. Ma, L.-P. Ma, Z. Zhang, Q. Fu, L.-M. Peng, X. Bao and H.-M. Cheng, *Nat. Commun.*, 2012, **3**, 1.
13 C. J. L. de la Rosa, J. Sun, N. Lindvall, M. T. Cole, Y. Nam, M. Loffler, E. Olsson, K. B. K. Teo and A. Yurgens, *Appl. Phys. Lett.*, 2013, **102**, 022101.
14 L. G. P. Martins, Y. Song, T. Zeng, M. S. Dresselhaus, J. Kong and P. T. Araujo, *Proc. Natl. Acad. Sci. U. S. A.*, 2013, **110**, 17762.
15 A. G. Starodubov, M. A. Medvetskii, A. M. Shikin and V. K. Adamchuk, *Phys. Solid State*, 2004, **46**, 1340.
16 J. Vaari, J. Lahtinen and P. Hautojarvi, *Catal. Lett.*, 1997, **44**, 4349.
17 H. Ueta, M. Saida, C. Nakai, Y. Yamada, M. Sasaki and S. Yamamoto, *Surf. Sci.*, 2004, **560**, 183190.
18 J. Coraux, A. T. Ndiaye, C. Busse and T. Michely, *Nano Lett.*, 2008, **8**, 565570.
19 A. L. V. de Parga, F. Calleja, B. Borca, J. M. C. G. Passeggi, J. J. Hinarejos, F. Guinea and R. Miranda, *Phys. Rev. Lett.*, 2008, **100**, 0568074.
20 R. Saito, A. Jorio, A. G. Souza Filho, G. Dresselhaus, M. S. Dresselhaus and M. A. Pimenta, *Phys. Rev. Lett.*, 2002, **88**, 027401.
21 L. H. Hess, M. V. Hauf, M. Seifert, F. Speck, T. Seyller, M. Stutzmann, I. D. Sharp and J. A. Garrido, *Appl. Phys. Lett.*, 2011, **99**, 033503.
22 M. Dankerl, M. V. Hauf, A. Lippert, L. H. Hess, S. Birner, I. D. Sharp, A. Mahmood, P. Mallet, J.-Y. Veuillen, M. Stutzmann and J. A. Garrido, *Adv. Funct. Mater.*, 2010, **20**, 3117.